Non-Destructive Study of Thermal Dissipation in Shape Memory Alloy Hybrid Composite Systems

D. Bollas[1], J. Parthenios[1,2] and C. Galiotis[1,2]

[1] Institute of Chemical Engineering and High Temperature Chemical Processes
Foundation of Research and Technology-Hellas
P.O. BOX 1414, Patras 265 04, Greece
[2] Material Science Department
University of Patras, 265 04 Patras
e-mail: c.galiotis@iceht.forth.gr

Abstract: Smart hybrid systems incorporating Shape Memory Alloy (SMA) wires as mechanical actuators and aramid fibres as spectroscopic sensors have been investigated. Two SMA wires identical in length have been integrated in the composite specimens examined; one unprestrained and the other prestrained by 3%. The SMA wires were connected in series and resistively activated at four elevated temperature levels. The resultant temperature distributions were recorded simultaneously by two independent methods. The first is based on the capability of the aramid fibres to act as stress and/or temperature Raman sensors, while the other one was based on the thermal trace of the surface specimen, which was recorded by a thermal imaging camera. The scope of this work is two-fold; (a) to assess the capability of the aramid fibres to act as temperature and/ or stress sensors in SMA hybrid composite materials, in an inhomogeneous thermal and/or stress field and (b) to combine two independent non-destructive methods for measuring temperature with high spatial resolution. We conclude that the aramid fibres can be used adequately as temperature sensors and by combining these two independent methods the stress field that is developed within a composite system incorporating thermally activated SMA wires can be effectively determined.

1. Introduction

The term "smart" refers to a relatively new and emerging class of materials and/ or systems, which are under continuous development during the last 15 years. These are materials or material systems which, imitating some biological systems, exhibit the ability to modify some of their properties (shape, Young Modulus, damping capacity), under the influence of an external stimulus. In order to manifest such a performance, these material systems should integrate three functionalities: i) sensing, that gives the system the ability to sense the stimuli, ii) actuation, which enables the structure to change its property/ies and iii)control of the sensing and actuation functions [1].

A subclass of "smart" materials consists of systems that are able to change their shape in a controllable way. The so-called *morphing* functionality can be added to the system by incorporating actuators with the ability to undergo large recoverable deformations. The materials that offers this capability are the Shape Memory Alloys (SMA), which are mainly binary NiTi or ternary NiTiX (where X could be Cu, Co, Fe, Nb etc.) alloys and can recover deformations up to 10% due to the "Shape Memory Effect". This Effect is associated to a reversible crystallographic deformation, namely martensitic transformation, between two crystal formations, the martensitic and the austenitic one. At relatively low temperatures, the SMA material is a low ordered martensite, able to sustain large plastic deformations. Nevertheless, at relatively high temperatures, the same material transforms to a high ordered martensite, regaining its original shape. The temperatures at which these transformations take place, known as M_s, M_f, A_s and A_f (where M stands for Martensite, A for Austenite and the subscripts s and f declare the start and finish of the transformations), depend on the composition and treating of the SMA material [2].

Hence, SMA materials in the form of thin wires can generate compressive stresses under constrain conditions where they are prevented from regaining their original shape during

martensitic transformation [2]. Over the last 10 years many research attempts have propose the integration of prestrained SMA wires in fibre reinforced polymer matrix composites leading to a hybrid material system capable to manifest the *morphing* functionality [1,2]. Some of them [3,4,5] has been proved unsuccessful [6], while only recently the shape change in a large scale systems incorporating SMA wires has been realised [7,8,9]. In the meanwhile, great advance has been achieved towards comprehending the mechanisms of the stress generation by constrained SMA materials during their activation and the governing parameters [10,11]. Additionally, a new methodology has been proposed for exploiting the sensing capability of aramid fibres for determining stress and temperature distribution in hybrid composites incorporating prestrained SMA wires by means of Raman Microscopy[7,8,12,13,14].

In the present work hybrid composite systems, consisting of an epoxy resin matrix, reinforced by aramid fibres, incorporating SMA wires, are examined. By exploiting the temperature sensing capability of aramid fibres, we record the temperature distributions developed by two thermally activated SMA wires using Raman Microscopy. One wire is unprestrained while the other is subjecting to a tensile strain of 3%. The wires are resistively activated at four different temperature levels. Simultaneously, temperature distributions are recorded using a thermal imaging camera. By comparing the results by these two independent "thermometers", the stress distributions developed by the two SMA wires are extracted.

2. Experimental

The hybrid composite specimen was produced under autoclave conditions. It consists of two SMA wires placed in between two plies of Kevlar fibre (53.5 %) / epoxy resin unidirectional prepreg tapes, with a 0.5 mm total width. SMA wires were ternary NiTiCu (44/44/12 % wt.) with 150 μm in diameter, supplied by Memry Co., U.S.A.. One of the SMA wires was unprestrained, while a 3% prestrain was imposed to the other, and were separated by 5 cm which is adequate for preventing the inter-wire interaction. Du Pont de Nemours Inc. produced the Kevlar 29 fibres with diameter of 16 μm, and Advanced Composites Group, UK, supplied unidirectional prepreg tapes. Details concerning the choice of the materials along with the preparation of the specimens and the curing process, can be found elsewhere [7,8]. Nevertheless it should be noticed that the use of a special designed frame was necessary for keeping the prestrain of the wire during the autoclave procedure, while the curing process leads to a higher Tg for the resin than the activation temperatures of the SMA wires.

The Raman spectra were recorded normal to the direction of the wires, with a step more or less equal to the diameter of the aramid fibres, during the wires' activation. The shift of the 1611 cm^{-1} band of the Raman spectra of the Kevlar 29 fibre, which corresponds mainly to ring/C–C stretching of the aromatic groups which are placed on the skeletal backbone of the molecular chain, was recorded [15]. This mode shifts to lower wavenumbers under tensile deformation and temperature and to higher values under compressive deformation. The relationships of wavenumber shifts as a function of stress or temperature are linear with slopes of -4.0 ± 0.5 cm^{-1}/GPa or -0.015 ± 0.001 $cm^{-1}/^{o}C$ respectively. It is worth noting here that the band shift is referred to the change of band position as compared to the corresponding values the free-standing fibres in air. The nominal activation temperature levels were equal to 40, 60, 80 and 100 ^{o}C and were determined by a suitable thermocouple situated at the surface of the specimen and above the unprestrained SMA wire. Simultaneously to the spectra acquisition, a thermal imaging camera equipped with a close – up lens, which yielded a spatial resolution of 25 μm, was used for recording the temperature profiles developed at the

specimen surface. More details concerning the experimental set – up (Fig. 1) are given in detail elsewhere [6,7,8].

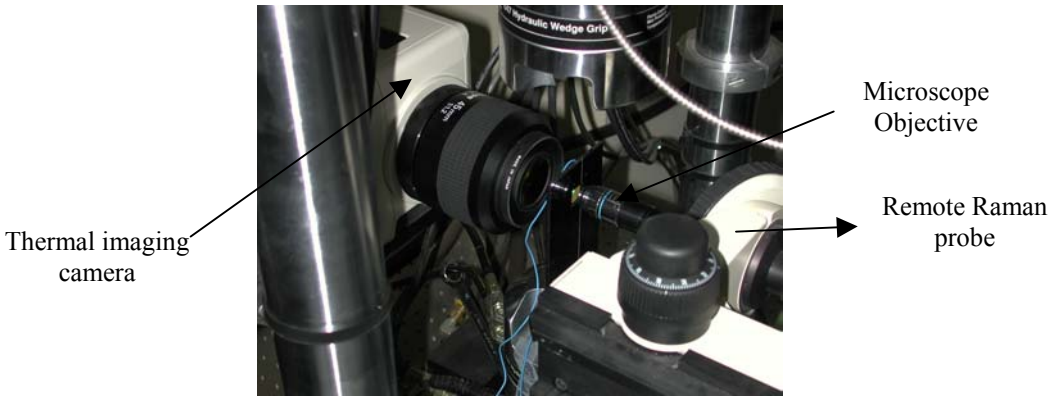

Fig. 1 Experimental set-up

3. RESULTS

The wavenumber shift of the 1611 cm^{-1} Raman band of Kevlar 29 fibre, as a function of the distance from each SMA wire, are presented at Figs. 2 and 3, respectively. The positions of the two SMA wires are also shown in these Figures. As it was expected, at each temperature level and for both of the wires, the shift of the 1611 cm^{-1} band has its maximum for fibres above the wires, while there is a near exponential decay as the distance from the wires is increased. Also, the shifts of this band at ambient temperature (25 ^{o}C), which correspond to the residual thermal stresses developed within the composite during manufacturing, are of the order of 0.30 cm^{-1} for both wires. In addition, by increasing the temperature activation level, there is also an increment on the shift of the 1611 cm^{-1} band. Nevertheless, in the case of the unprestrained SMA wire, the shifts of the recorded wavenumber mode appear to be higher, especially at the vicinity of the SMA wires. This difference is slight at the activation temperature of 40 ^{o}C and is gradually rising, from approximately -0.28 cm^{-1} at the level of 60 ^{o}C, to 0.35 cm^{-1} at the level of 80 ^{o}C, reaching its maximum of 0.40 cm^{-1} at 100 ^{o}C. Furthermore, there is a clear tendency of the wavenumber shifts at all cases of the SMA wires' activation to reach the corresponding values of the shift of the 1611 cm^{-1} band recorded at the 25 ^{o}C, at distances far away from the heat source (wire).

At Figs 4 and 5 the temperature distributions as a function of the distance from each wire, recorded by the thermal imaging camera, are given. It should be mentioned here that the emmissivity of the surface of the specimen was considered to be uniform and estimated as 0.89, using a thermocouple that was situated on this surface and at a distance from the two wires. As it was expected, the maximum of the temperature appears to be above the SMA wires for both cases. A difference between the temperatures recorded by the thermal imaging camera and the temperature activation levels defined by the thermocouple is evident. This difference is imperceptible at the first activation level, while it is gradually rising, as the activation level is increasing. Furthermore, there is a difference between the temperatures recorded at each activation level, for the two SMA wires. At the first level the peak of both temperature distributions is equal to 41 ^{o}C, at the second one the maximum temperature for the unprestrained wire is equal to 65 ^{o}C while for the prestrained one is equal to 74 ^{o}C. At the third activation level the maximum temperature for the first wire is equal to 94 ^{o}C and for the second one 104 ^{o}C, while at the last activation level the peaks of the temperature appears to be 119 and 136 ^{o}C, respectively. It is also clear that for both wires and at all the activation levels, the temperature tends to reach a constant value away from the wires.

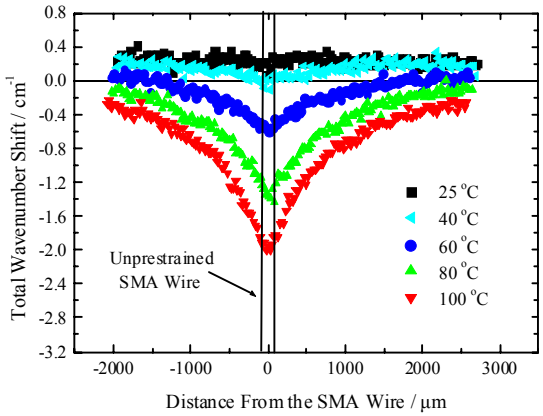

Fig. 2 Spatial distribution of wavenumber shift of the 1611 cm^{-1} normal to the un-prestrained wire direction

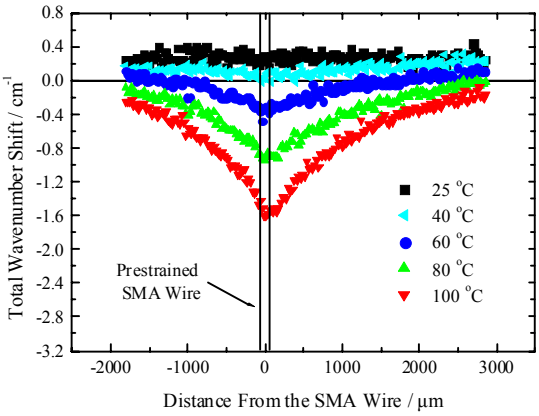

Fig. 3 Spatial distribution of wavenumber shift of the 1611 cm^{-1} normal to the prestrained wire direction

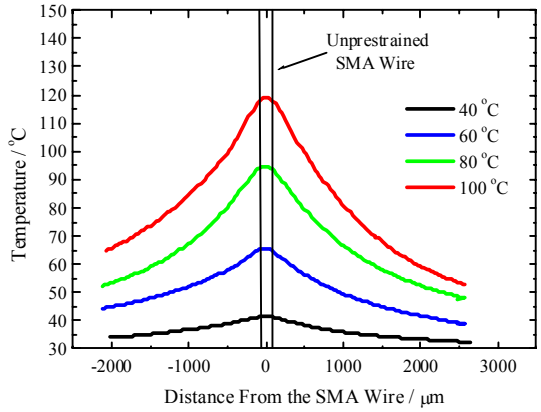

Fig. 4 Spatial distribution of temperature recorded by thermal imaging camera, normal to the un-prestrained wire direction

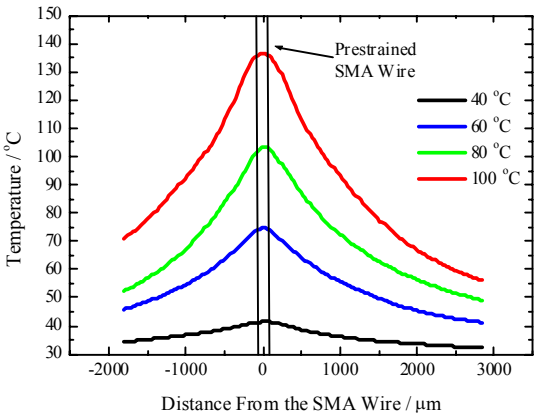

Fig. 5 Spatial distribution of temperature recorded by thermal imaging camera, normal to the prestrained wire direction

In Figs 6 and 7 the wavenumber shift of the 1611 cm^{-1} band due to the thermal and stress fields generated by the activation of the SMA wires are presented by the experimental points for both of the wires. By converting the temperature distributions recorded by the thermal imaging camera to shifts of the 1611 cm^{-1} band produced the lines, which are presented also at these two Figures. It is clear that for the unprestrained wire there is no coincidence between the shifts of the 1611 cm^{-1} band, except for the case of the first activation level. There is a difference equal more or less to 0.24, 0.59 and 0.86 cm^{-1} at the activation temperature of 60, 80 and 100 C^{o}, respectively. On the contrary, for the prestrained wire, there is a clear coincidence between the wavenumber shift of the 1611 cm^{-1} band recorded by means of Raman spectroscopy, with the corresponding shift produced using the temperature distributions recorded by the IR camera.

It is feasible for someone to understand that the difference between the shifts of the 1611 cm^{-1} band derived with the two methods described above, could be attributed to the stress field generated from the SMA wires during their activation. Transmitted stresses were calculated by deconvoluting the derived thermal wavenumber shift (Fig. 6) from the total wavenumber shift distribution (fig.2). The results are shown in Fig. 8, for the unprestrained wire, where it is clear that at the activation levels of 60, 80 and 100 ^{o}C tensile stresses are been transmitted to Kevlar 29 fibres through the resin matrix, the values of which have their maximums above the wire, while they are gradually decreased to zero. It is also obvious that at elevated

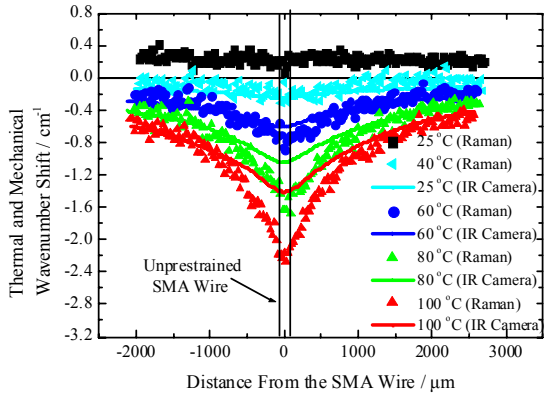

Fig. 6 The spatial distribution of wavenumber shift of the 1611 cm^{-1} normal to the un-prestrained wire direction and the converted temperature to thermal shift

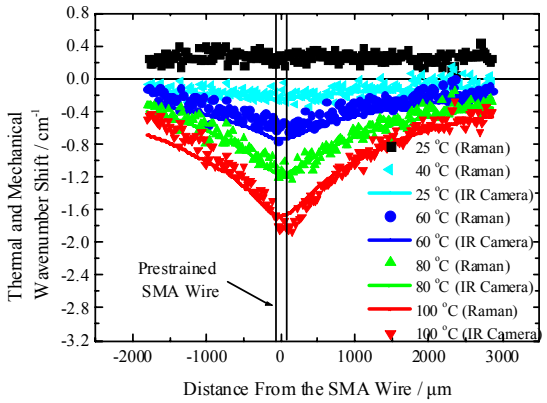

Fig. 7 The spatial distribution of wavenumber shift of the 1611 cm^{-1} normal to the prestrained wire direction and the converted temperature to thermal shift

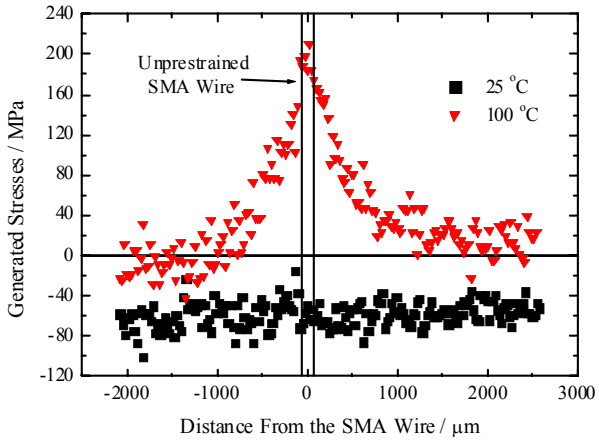

Fig. 8 The distribution of transmitted fibre stresses, normal to the un-prestrained wire direction

activation levels, the maximum stresses are become higher. So, while the mean value of the residual stresses is around -60 MPa, at 40 °C some short of compressive stresses seems to be generated from the wire. At the next activation level, the maximum of the generated stresses is around 60 MPa, at the level of 80 °C this maximum is almost equal to 140 MPa, while at the highest activation level this maximum reaches the value of 200 MPa.

3. DISCUSSION

As it is depicted in Figs 2 and 3, the maximum of the total wavenumber shift of the 1611 cm^{-1} band appears to be above the two SMA wires. This was expected, since the wires act as heat and stress generators during their activation. The difference between the maximums of these wavenumber shifts above the two wires, which is gradually increasing as the level of the activation is becoming higher, indicates that there is a difference between the thermal fields, the stress fields or at both of these fields which are developing during the activation of the two SMA wires. Apart from that, for both of the two cases and for all the activation levels, the tendency of the shifts of the 1611 cm^{-1} band to reach its corresponding values attributed to the residual thermal stresses of the specimen far away from the two wires, is a strong indication that the used methodology stands.

Regarding the differences between the maximums of the temperatures recorded using the IR imaging camera, shown at Figs 4 and 5, with the corresponding values recorded by the thermocouple above the unprestrained SMA wire, that is the so-called level of activation temperature, could be attributed mainly to three reasons. First of all, the thermocouple is

"sensing" the temperature at the surface of the specimen, while the IR technique makes use of the radiation that is transmitted from the whole body of the specimen. Furthermore, there is always the possibility that the thermocouple is not attached perfectly on the surface of the specimen. At last, the emmissivity of the surface of the specimen may not be uniform, especially above the wires and for elevated temperatures, since these wires act as temperature generators. Regarding the differences of the recorded temperature between the two SMA wires at each activation level, there is only one rational explanation. Providing that the two SMA wires were connected in series, that is the same amount of current were passing through them at the same period of time, the different amount of the generated heat can be attributed to their different specific resistances. The unprestrained SMA wire was at the austenitic crystallographic phase, while part of the prestrained wire was at the austenitic situation and part of it at the martensitic one [10].

Concerning the results shown at Figs 6 and 7, where the shifts of the 1611 cm^{-1} band as these were assessed by the laser Raman technique are compared to those derived by converting the temperature profiles recorded by the IR camera to shifts of this band, it could be concluded that the unprestrained wire produces stresses, while the prestrained wire is not. It is also clear from Fig. 6 that the difference between these two shifts is positive, so one must expect that the above-mentioned stresses are tensile ones, since the 1611 cm^{-1} wavenumber mode shifts to higher values with tension. This is even more obvious at Fig 8, where the pre-mentioned differences have been converted to generated stresses. As it was expected there are tensile stresses transmitted from the SMA wire to the Kevlar fibres, which can be attributed to the positive thermal expansion coefficient of the wire. So, by thermally activating the SMA wire, it expands, generating tensile stresses within the composite.

As far as the prestrained wire is concerned, the close coincidence of thermal and total wavenumber shift distributions, shown in Fig. 7, proves that there are no stresses transmitted from the prestrained wire to the aramid fibres. This can be explained as follows: Due to the thermal expansion coefficient of the SMA, it generates tensile stresses as for the unprestrained wire. On the other hand, during activation compressive stresses are generated due to the Shape Memory Effect. It seems that these two effects are contradictory leading to a balance of stress inside the composite.

4. Conclusions

A "smart" hybrid composite system was manufactured under autoclave conditions, incorporating two SMA wires, one unprestrained and one with a prestrain equal to 3 %, into an epoxy resin matrix reinforced by Kevlar 29 fibres. The two SMA wires were connected in series and they were activated at different temperature levels by electrical current. The thermal dissipation developed within the composite during this activation was recorded in real time using two non-destructive, independent methods. The first one was based on the potentiality of the Kevlar 29 fibres to be used as temperature sensors by means of laser Raman spectroscopy, while for the second one an IR imaging camera was used. The results indicate that, there is a difference between the values of the temperature as these were recorded by the thermal imaging camera, to those recorded by the thermocouple, which also was used to determine the temperature activation levels. This is possible due to the difference of the nature of these two methods, as well as to possible problems associated to the placing of the thermocouple or the definition of the emmissivity of the surface of the specimen. Furthermore, the combination of the Raman spectroscopy with the IR imaging, indicates that tensile stresses are generated from the unprestrained SMA wire during its activation, probably because it expands due to its positive thermal expansion coefficient. On the contrary, for the

case of the prestrained SMA wire, it seems that as a whole there is not a generation of any kind of stresses during its activation. This can be attributed to the generation of compressive stresses because of the Shape Memory Effect, which counterbalance the tensile stresses that are generated because of its positive thermal expansion coefficient.

Acknowledgements

We would like to thank the GRST (General Secretariat for Research and Technology), of the Ministry of Development of Greece, for funding part of this work under the frame of the PENED Project (programme code: 01ED 363).

References

[1] **Gandhi, M.V.** and **Thompson, B.S.**, "Smart Materials and Structures", 1st Edition, Chapman and Hall, London (1992)

[2] **Duering, T.W., Melton, K.N., StÖckel, D.** and **Wayman, C. M.**, "*Engineering aspects of shape memory alloys*", Butterworth-Heinemann, London, 1990.

[3] **Liang, C., Jia, J.** and **Rogers, C.**, "Behavior of shape memory alloy reinforced composite plates part ii: Results.", *Proceedings of the 30th Structures, Structural Dynamics and Materials Conference* (1989) number AIAA-89-1331-CP: 1504-1513.

[4] **Rogers, C.A.**, "Active vibration and structural control of shape memory alloy hybrid composites: Experimental results", *J. of Acoustical Society of America*, **88**/6 (1990), 2803-2811.

[5] **Jonnalagadda, K.D.**, **Sottos, N.R.**, **Qidwai, M.A.** and **Lagoudas, D.C.**, "Transformation of Embedded Shape Memory Alloy Ribbons", *J. of Intell. Mat. Sys. and Struc.,* **9**/5 (1998), 379-390.

[6] **Psarras, G.C.**, **Parthenios, J.**, **Bollas, D.** and **Galiotis, C.**, "Internal stress generation in composites incorporating prestrained Shape Memory Alloy wires", *Proceedings of the 10th European Conference on Composite Materials* (2002), available on CD-ROM.

[7] **Psarras, G.C., Parthenios, J.** and **Galiotis, C.,** "Adaptive composites incorporating shape memory alloy wires Part I Probing the internal stress and temperature distributions with a laser Raman sensor", *J. of Mat. Sci.*, **36** (2001), 535-546.

[8] **Parthenios, J., Psarras, G.C.** and **Galiotis, C.**,"Adaptive composites incorporating shape memory alloy wires Part 2: development of internal recovery stresses as a function of activation temperature", *Comp. Appl. St. Manuf.*, **32** (2002), 1735-1747.

[9] **Schrooten, J., Michaud, V., Parthenios, J., Psarras, G.C., Galiotis, C., Gotthard, R., Manson, J.A.** and **Humbeeck, J.V.**, "Progress on Composites with Embedded Shape Memory Alloy wires", *Mat. Trans.*, **43**/5 (2002), 961-973.

[10] **Zheng, Y.J., Schrooten, J., Tsoi, K.A.** and **Stalmans, R**., "Thermal response of glass fibre/epoxy composites with embedded TiNiCu alloy wires", *Mat. Sci. and Eng. A*, **335** (2002), 157-163.

[11] **Sittner, P., Michaud, V., Balta-Neuman, J.A.** and **Schrooten, J.**, "Modelling and Material Design of SMA Polymer Comosites", *International Symposium on Smart Materials, PRICM4*, (2001).

[12] **Vlattas, C.**, "A Study Of The Mechanical Properties Of Liquid Crystal Polymer Fibres And Their Adhesion To Epoxy Resin Using Laser Raman Spectroscopy", *PhD Thesis*, Materials Department, Queen Mary and Westfield College, Faculty of Engineering of the University of London, London (1995).

[13] **Galiotis, C.**, in Micromechanics of Reinforcement Using Laser Raman Spectroscopy (in Microstructural characterisation of fiber – reinforced composites, J. Summerscales), Woodhead pub. Co. (1998).

[14] **Psarras, G.C., Parthenios, J., Bollas, D.** and **Galiotis, C.,** "Stress and Temperature Self-Sensing Fibres", *Chem. Phys. Lett.*, **367**/3-4 (2003), 270 – 277.

[15] **Kim, P.K., Chang, C.** and **Hsu, S.L.**, "Normal vibrational analysis of a rigid rod polymer: poly(p-phenylene terephthalamide", *Polymer*, **27** (1986), 34-46.